Optical Engineering

SPIEDigitalLibrary.org/oe

Optical sensor for reducing influence of intensity fluctuations on output stability

Vladimir Ya. Mendeleyev
Andrei V. Kourilovitch

SPIE

Optical sensor for reducing influence of intensity fluctuations on output stability

Vladimir Ya. Mendeleyev* **and Andrei V. Kourilovitch**
Joint Institute for High Temperatures of Russian Academy of Sciences, Izhorskaya 13 bd. 2, Moscow 125412, Russia

Abstract. High-precision optical measurements depend on the optical sensor's stability. Light source's intensity fluctuations are the dominant cause for output instability of the sensor. In order to address this issue, we have developed an optical sensor for reducing influence of the intensity fluctuations on the output stability. The sensor comprises a light source generating smoothly modulated intensity, a measuring channel, a reference channel, and a beam splitter dividing the light source intensity between the channels. The reference channel opens the measuring channel when the light source intensity equals a specific value and the measuring channel converts the input intensity into the output of the sensor. The sensor was designed and studied experimentally at a wavelength of 635 nm and a modulation frequency of 285 Hz. With the sensor, the influence of the intensity fluctuations on the output stability was reduced 110 times and the relative rms instability of 4.5×10^{-5} was obtained. Techniques to achieve the instability of 1.0×10^{-5} are also shown. [DOI: 10.1117/1.OE.53.2.027106]

Keywords: optical sensor; light source; intensity fluctuations; output stability.

Paper 131533 received Oct. 6, 2013; revised manuscript received Jan. 28, 2014; accepted for publication Feb. 3, 2014; published online Mar. 3, 2014.

1 Introduction

Technologies utilized in current laser gyroscopes, microelectromechanical systems, and cavity ring-down techniques require mirrors with a reflectance of ~0.9999.[1–3] Such reflectance can be achieved in multilayer dielectric mirrors manufactured with direct monitoring.[4] During the process of manufacturing, *in situ* measurements are taken to calculate optical properties of the layer deposited on the substrate. This allows to compensate for the manufacturing errors in the current layer with the subsequent one. For the optical measurements, a major issue is to provide long-term output stability of the optical sensor despite fluctuations of light source intensity.[5]

To stabilize an output of the optical sensor, the feedback methods[6–14] and the ratio method[15–24] are used. The sensors based on these methods comprise a light source, a measuring channel, a reference channel, a compensation channel, and a beam splitter dividing the light source intensity between the reference channel and the measuring one. Detector-amplifier units of the measuring and reference channels convert the input intensities into analog signals. If the input intensity of the measuring channel is small, a modulator of the light source intensity and the lock-in-amplifier are optionally used to increase signal-to-noise ratio at the channel's output. The reference channel tracks fluctuations of the light source intensity and controls the compensation channel to stabilize the output of the sensor. The compensation channel of the sensors based on the feedback methods controls either the intensity of the light source[6–10] or the sensitivity of the measuring channel.[11–14] In the sensors based on the ratio method, the compensation channel defines the output of the optical sensor as a ratio between the outputs of the measuring and reference channels. The low limit of the relative rms output instability achieved with the optical sensors based on the above methods was $>1.0 \times 10^{-4}$ for ~1 h.[9,15]

There are two problems to overcome the instability limit achieved with the mentioned sensors. The first problem implies that the conversion of the input intensity into the analog output in the measuring channel and that in the reference one are not fully identical. Because of that, the same fluctuations of the light source intensity cause different variations of the analog outputs in both reference and measuring channels. The second problem relates to compensation of the output instability caused by the intensity fluctuations. It implies that the compensation should take into account the difference between the conversion of the light intensity into the analog output in the reference channel and that in the measuring one. In the feedback methods, the compensation should also take into account nonlinear dependence of the light source intensity and the measuring channel sensitivity on the output of the compensation channel.

To overcome the above stability limit, a new optical sensor was developed. This sensor comprises a light source generating smoothly modulated intensity, a measuring channel, a reference channel, and a beam splitter. The compensation channel is not utilized in the sensor. The beam splitter and detector-amplifier units of the measuring and reference channels operate in the same way as mentioned above. In the reference channel, the analog output and voltage of a high stability voltage reference are compared. At a moment of time when the analog output equals the reference voltage, the reference channel opens the measuring channel and the input intensity of the measuring channel is converted into the output of the sensor. Note that the output of the reference channel's detector-amplifier unit is acquired at the same specific value of the light source intensity. Therefore

*Address all correspondence to: Vladimir Ya. Mendeleyev, E-mail: v_mendeleyev@list.ru

the detector-amplifier unit of the reference channel is not required to be identical to that of the measuring channel.

Said specific value of the light source intensity depends only on the reflectance of the beam splitter, the conversion factor of the reference channel's detector-amplifier unit, and the reference voltage. If the reflectance, the conversion factor, and the reference voltage are stable, the specific intensity should be stable too. Since the measuring channel converts the input intensity into the output of the sensor at the specific intensity, the intensity fluctuations of the light source should not influence the output stability of the sensor.

This paper describes the design of the developed sensor, the principle of the stabilization, and study of the sensor's stability.

2 Design of Sensor

A schematic diagram of the sensor is shown in Fig. 1. A light source comprises a semiconductor laser diode, a sinusoidal current driver, a lens (1), a diaphragm (2), and a Glan prism (3) stabilizing polarization of the light source's beam. The beam is divided by a beam splitter (4) into two. The first beam passes through a neutral density filter (5), is reflected from a smooth steel surface (6), and falls onto a detector (7). The second beam falls onto a detector (8). Both outputs of the detectors go through preamplifiers and amplifiers. The leading edge of a pulse generated by a comparator occurs when the output of the reference channel amplifier equals a specific reference voltage. The pulse and an output of the measuring channel amplifier go to an analog-to-digital converter (ADC) comprising a gate, a capacitor, and a successive approximation register (SAR). The gate is opened by the leading edge of the pulse and the capacitor samples a part of the output of the measuring channel amplifier. Then SAR converts the capacitor charge into the digital output of the sensor.

Figure 2 shows the design of the sensor. A semiconductor laser diode LCU633541A ($\lambda = 635$ nm) and the laser driver operating at the frequency $f = 285$ Hz were utilized in the light source. The laser diode, the driver, and the lens were mounted in a single unit. Precision Hamamatsu detectors S1226-8BK, high-precision and low-noise preamplifiers AD 8512, and amplifiers OPA 2228 were used in the reference and measuring channels. The S1226-8BK detectors have photosensitive area of 5.8×5.8 mm, a photosensitivity of $\sim$0.33 A/W at the wavelength of 635 nm, and a rise time of 2 μs. An ultraprecision and low-noise voltage reference ADR420, a comparator LMC7211, and a 16-bit ADC ADS8515 were also used in the sensor. The sampling time for the ADC capacitor was 2 μs. The output of the optical sensor was obtained by averaging the ADC outputs for time of $100/f$. This helped to reduce the dependence of the sensor's stability on noise caused by the detectors and the electronics. To prevent temperature instability of the electronics, the computer was located as far away as possible.

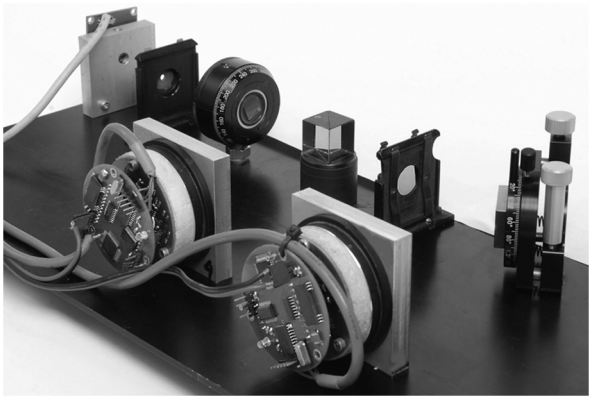

Fig. 2 Design of the sensor.

3 Principle of Stabilization and Estimation of Instability

In this section, the analysis of the stabilization principle is performed assuming that the contribution of the intrinsic noise of the detectors and electronics to the output of the sensor is negligible in comparison to that of the light source's intensity fluctuations.

The principle of the stabilization is illustrated by Fig. 3 showing the output $U_1(t)$ of the reference channel amplifier, the output $U_2(t)$ of the measuring channel amplifier, the reference voltage U_0, the comparator pulses $U_p(t)$, and the charges $U_c(t_i)$ of the capacitor.

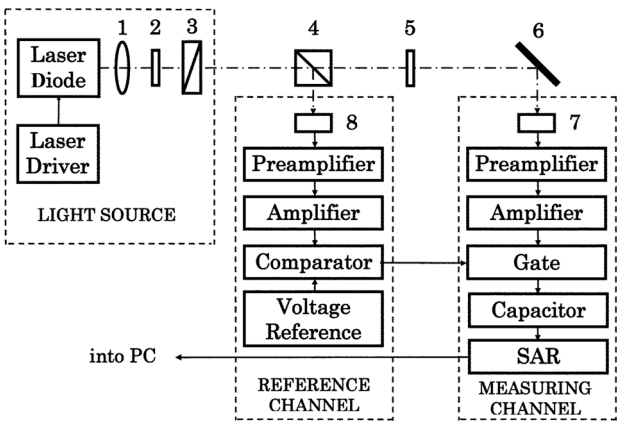

Fig. 1 Schematic diagram of the sensor. (1) Lens. (2) Diaphragm. (3) Glan prism. (4) Beam splitter. (5) Neutral density filter. (6) Smooth steel surface. (7) and (8) Detectors.

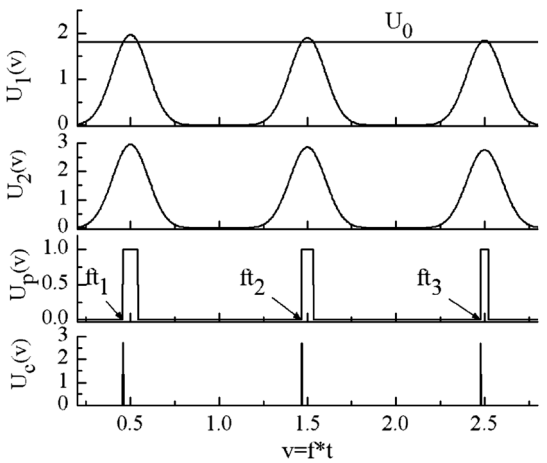

Fig. 3 Signals internal to the optical sensor.

The $U_1(t)$ and $U_2(t)$ outputs are described as

$$U_1(t) = I(t)\rho_{\text{bs}}\eta_1 \tag{1}$$

$$U_2(t) = I(t)\xi_{\text{bs}}\xi_d R\eta_2, \tag{2}$$

where t is the current time, $I(t)$ is the modulated intensity of the light source, ρ_{bs} is the reflectance of the beam splitter, η_1 and η_2 are the conversion factors defined as the ratio between the output of the amplifier and the light intensity on the detector; ξ_{bs} is the transmittance of the beam splitter; ξ_d is the transmittance of the neutral density filter, and R is the reflectance of the smooth steel surface. Decrease in the amplitude of the $U_1(t)$ and $U_2(t)$ functions simulates instability of the light source intensity. The shape of the functions resembles the shape of the analog outputs of the amplifiers and is described by the $I(t)$ function showing nonlinear response of the laser diode's optical output versus the sinusoidal current of the driver.

$$I(t) = I_0\{1-\alpha\text{FIX}[(f\times t)]\}(0.5\{1+\cos[2\pi(f\times t-0.5)]\}) \times\exp(-\{3.2\pi[f\times t-0.5-FIX(f\times t)]\}^2), \tag{3}$$

where I_0 is the amplitude of the intensity at $t = 0.5/f$, α is the index of the amplitude variation caused by the intensity instability, and FIX is the function[25] that returns the integer part of the $f\times t$ product.

In Fig. 3, t_i moments of time ($i = 1$, 2, and 3) correspond to equality between the $U_1(t)$ outputs of the reference channel amplifier and the U_0 reference voltage.

$$U_1(t_i) = U_0, \tag{4}$$

where $t_i = (i-0.5)/f - \tau_i/2$; τ_i is the duration of the comparator pulses corresponding to $i = 1$, 2, and 3. From Eqs. (1) and (4), it is clear that the light source intensity at the t_i moments of time has a constant specific value defined as

$$I(t_i) = U_0/\rho_{\text{bs}}\eta_1. \tag{5}$$

At these moments, the leading edges of the comparator pulses $U_p(t)$ open the gate and the capacitor samples the $U_2(t)$ outputs of the measuring channel amplifier. The $U_c(t_i)$ charge of the capacitor is described as

$$U_c(t_i) = \int_{t_i}^{t_i+\tau_s} U_2(t)\text{d}t, \tag{6}$$

where $\tau_s = 2$ μs is the sampling time of the ADC capacitor. The charge described by Eq. (6) is converted by the SAR into the digital output $U_c^*(t_i)$ of the optical sensor. The described procedure shows that the outputs of the optical sensor are generated at the same specific intensity $I(t_i)$ of the light source and their stability should not depend on the intensity fluctuations.

However, as we can see from Fig. 3, the amplitude instability of the $U_1(t)$ outputs caused by the intensity fluctuations makes the t_i moments drift against the $(i-0.5)/f$ ones. Therefore, behavior of the $U_2(t)$ output is different for the different $[t_i, t_i+\tau_s]$ intervals, and the $U_c(t_i)$ value is not stable. It means that the output amplitude instability δU_2 of the measuring channel amplifier affects the output instability ΔU_I of the optical sensor.

The relative instabilities δU_2 and ΔU_I were calculated from the equation[26]

$$\Delta = (U_{\max} - U_{\min})/(U_{\max} + U_{\min}). \tag{7}$$

To calculate the δU_2 instability, the variables Δ, $U_{\max}$, and $U_{\min}$ in Eq. (7) were substituted with δU_2, $U_{2\,\max} = I_0\xi_{\text{bs}}\xi_d R\eta_2[1+\alpha]$, and $U_{2\ \min} = I_0\xi_{\text{bs}}\xi_d R\eta_2[1-\alpha]$, respectively, and $\delta U_2 = \alpha$ was obtained. To calculate the ΔU_I instability, the variables Δ, $U_{\max}$, and $U_{\min}$ in Eq. (7) were substituted with ΔU_I, $U_{c\,\max}$, and $U_{c\,\min}$, respectively, and the values of $U_{c\,\max}$ and $U_{c\,\min}$ were calculated using Eqs. (1) to (6). In these calculations, the α index was varied from 0.001 to 0.019 at $U_0 = 0.9U_1(t_1 = 0.5/f)$, the frequencies of 285 and 70 Hz, and the sampling time of 2 and 0.5 μs.

Figure 4 shows the dependence of the ΔU_I instability on the δU_2 instability, the f modulation frequency, and the τ_s sampling time. As we can see from Fig. 4, the ΔU_I instability increases with increasing the δU_2 instability and decreases with decreasing the f frequency and the τ_s sampling time. Such behavior of the ΔU_I instability is caused by the following. Decrease of the output amplitude instability, the modulation frequency, and the sampling time leads to decrease of influence of the analog output's shape on the charge of the ADC's capacitor. Because of that, the output stability of the sensor increases. Note that the lower limit of the modulation frequency depends on the conditions of an experiment. The lower limit of the sampling time depends on the conversion sensitivity of the ADC.

4 Experimental Study of Sensor

In this section, the output U of the sensor, its relative instability ΔU, and its relative rms instability σU are considered as values that depend on both the intensity fluctuations and the noise of the detectors and electronics. The sensor's instability was studied at $U_0 \approx 0.9U_1(t = 0.5/f)$ and two different light intensities on the detector of the measuring channel. Different neutral density filters were used to obtain these intensities.

4.1 *Experimental Results*

The long-term output instability of the optical sensor was characterized by the ΔU relative instability calculated from Eq. (7) and the σU relative rms instability calculated from the relation[26]

$$\sigma U = (1/U)\left\{[1/(M-1)]\sum_{m=1}^{M}(U_m - U)^2\right\}^{1/2}, \tag{8}$$

where U_m is the averaged output of the optical sensor determined with the period of 1 min, $U = (1/M)\sum_{m=1}^{M} U_m$, and $M = 60$; the $U_{\max}$ and $U_{\min}$ values were the maximum and minimum of the obtained U_m outputs.

The values $\sigma U = 4.6\times10^{-5}$ and $\Delta U = 1.1\times10^{-4}$ were measured at $U = 23{,}400.6$ obtained for the first neutral density filter. The values $\sigma U = 4.4\times10^{-5}$ and $\Delta U = 1.18\times10^{-4}$ were measured at $U = 1308.05$ obtained for the second neutral density filter. These data allow to conclude that

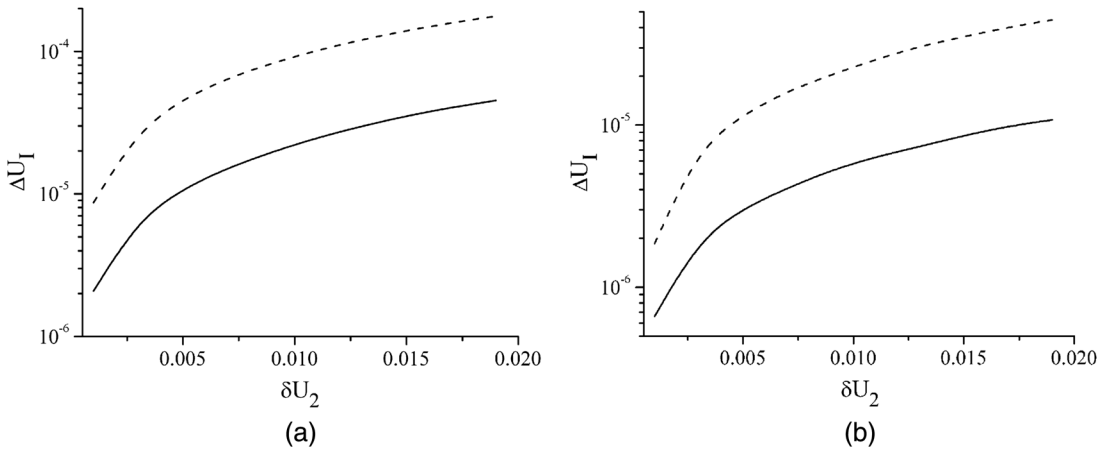

Fig. 4 (a) The relative output instability of the optical sensor versus the relative output instability of the measuring channel amplifier. The dashed line and the solid one correspond to the frequencies $f = 285$ Hz and $f = 70$ Hz, respectively, at the sampling time of 2 μs. The plots are satisfactorily described by the $\Delta U_I = A[\exp(-\delta U_2/t) - 1]$ function, where $A = 6.98 \times 10^{-3}$ and $t = -0.757$ at $f = 285$ Hz and $A = 1.4 \times 10^{-4}$ and $t = -0.067$ at $f = 70$ Hz. (b) The relative output instability of the optical sensor versus the relative output instability of the measuring channel amplifier. The dashed line and the solid one correspond to the frequencies $f = 285$ Hz and $f = 70$ Hz, respectively, at the sampling time of 0.5 μs. The plots are satisfactorily described by the $\Delta U_I = A[\exp(-\delta U_2/t) - 1]$ function, where $A = 8.9 \times 10^{-4}$ and $t = -0.388$ at $f = 285$ Hz and $A = -5.4 \times 10^{-4}$ and $t = 0.995$ at $f = 70$ Hz.

although the output of the optical sensor was varied almost 18-fold, (1) the $\sigma U/\Delta U$ ratios remained close to 0.4 and (2) the output stability of the optical sensor did not depend on the light intensity in the measuring channel.

Intrinsic noise of the detectors and the electronics was also determined experimentally at the sensor's output. In this experiment, an opaque screen was located before the photosensitive area of the measuring channel's detector. The relative rms noise σU_n was calculated from the equation

$$\sigma U_n = (1/U)\left\{[1/(Q-1)]\sum_{q=1}^{Q}(U_q - U_{n0})^2\right\}^{1/2}, \tag{9}$$

where U_q is the averaged output of the optical sensor determined with the period of 1 min, $Q = 10$, and $U_{n0} = (1/Q)\sum_{q=1}^{Q} U_q$.

The σU_n values were 5.98×10^{-7} and 1.07×10^{-5} for $U = 23{,}400.6$ and $U = 1308.05$, respectively.

To estimate contribution of the noise to the output instability, we assumed that the output instability caused by the intensity fluctuations and that caused by the noise are uncorrelated and the following equality is valid:

$$(\sigma U)^2 = (\sigma U_I)^2 + (\sigma U_n)^2, \tag{10}$$

where σU_I is the relative rms instability of the output caused by the intensity fluctuations.

The σU_I values estimated from Eq. (10) were 4.597×10^{-5} and 4.268×10^{-5} for $U = 23{,}400.6$ and $U = 1308.05$, respectively. Taking into account the criterion for negligible errors[27]

$$\sigma U < 1.05\sigma U_I, \tag{11}$$

we found that the contribution of the noise to the output instability can be neglected. This result allows the consideration that $\sigma U = \sigma U_I$ and $\Delta U = \Delta U_I$.

4.2 *Analysis*

Improvement in the output stability caused by reducing influence of the intensity fluctuations on the output of the sensor was defined as the ratio between the δU_2 output instability of the measuring channel amplifier and the ΔU output instability of the sensor. The δU_2 values were determined using Fig. 4 for the ΔU values obtained experimentally at $f = 285$ Hz and $\tau_s = 2$ μs. The improvement in the stability was ~110 for both intensities in the measuring channel.

The output instability described by the Allan variance $\sigma_y^2(M,T,\tau)$ was also estimated from the equation[28]

$$\sigma_y^2(M,T,\tau) = [1/(M-1)]\sum_{m=1}^{M}\left[\bar{y}_m - (1/M)\sum_{z=1}^{M}\bar{y}_z\right]^2, \tag{12}$$

where $\bar{y}_m = (Um - U)/U$, $T = 1$ min, $\tau = 100/f$, and M is the number of U_m measurements. The M value was varied from 10 to 60.

Plots of the $\sigma_y(M,T,\tau)$ rms variance as function of the M value are presented in Fig. 5 for $U = 23{,}400.6$ and $U = 1308.05$. As we can see from the figure, the $\sigma_y(M,T,\tau)$ values of both plots tend to constant value at $M \geq 55$. We assume that this constant value is average rms variance $\langle\sigma_y(M,T,\tau)\rangle$, where the $\langle\rangle$ brackets denote infinite time averaging.

The rms output instability σU of the optical sensor was also estimated at the modulation frequency of 70 Hz. The $\sigma U/\Delta U$ experimental value and the ΔU instability determined from Fig. 4 were used in the estimation. As follows from Fig. 4, change of the modulation frequency from 285 Hz down to 70 Hz reduces the ΔU instability down to 2.73×10^{-5}. Taking into account the $\sigma U/\Delta U$ experimental value, we obtained the σU estimate of $\sim 1.0 \times 10^{-5}$ at a frequency of 70 Hz and a sampling time of 2 μs. A similar result was obtained at a modulation frequency of 285 Hz and a sampling time of 0.5 μs.

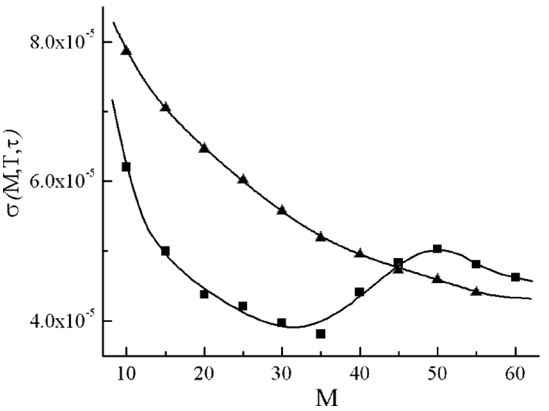

Fig. 5 Dependence of the rms variance on the number of measurements. Squares and triangles correspond to $U = 23,400.6$ and $U = 1308.05$, respectively.

The developed optical sensor belongs to the devices exhibiting long-term output stability. In Ref. 22, the rms repeatability of the measurement was $<3 \times 10^{-4}$ at the modulation frequency of 250 Hz. Measurements on Lambda 800 and 900 spectrophotometers[23] are performed at the modulation frequency of 46 Hz. The photometric peak-to-peak instability is $<2 \times 10^{-4}$. The same instability is obtained with Cary 4000, 5000, and 6000*i* spectrophotometers[24] at the modulation frequency of 30 Hz. In Ref. 15, the rms output instability of the order of 10^{-4} was achieved at the modulation frequency of 90 Hz. Therefore, we can assume that the low limit of the rms instability achieved by the commercially available products is of the order of 10^{-4} in the modulation frequency range of 30 to 250 Hz. We believe that the technical *solutions* suggested in our paper allow to obtain the rms instability of 10^{-5} at the modulation frequencies up to 285 Hz.

5 Summary

A sensor for reducing the influence of light source's intensity fluctuations on the output stability was developed, designed, and studied experimentally. The sensor comprises a light source generating smoothly modulated intensity, a measuring channel, a reference channel, and a beam splitter dividing the light source intensity between the reference channel and the measuring one. The sensor operated at a wavelength of 635 nm and a modulation frequency of 285 Hz. The reference channel opened the measuring channel when the light source intensity equals a specific value and the intensity in the measuring channel was converted into the output of the sensor for a sampling time of 2 μs.

The principle of stabilization was considered and influence of the intensity fluctuations on the output stability of the sensor was estimated for modulation frequencies of 285 and 70 Hz and sampling times of 2 and 0.5 μs. It was found that decrease of the modulation frequency and the sampling time leads to increase of the sensor's output stability.

The experiments were performed for two different intensities at the input of the measuring channel. Although the outputs of the sensor were varied almost 18-fold for the intensities used, the dependence of the output stability on the intensity was not found. The relative rms instability of the outputs was $\sim 4.5 \times 10^{-5}$ for 1 h. The noise of the detectors and the electronics was also estimated experimentally. It was found that the contribution of the noise to the output instability was negligible.

The improvement in the output stability of the sensor was estimated as the ratio between the output instability of the measuring channel's detector-amplifier unit and that of the sensor. It was ~110 for both intensities at the input of the measuring channel. Dependence of the rms variance on the number of measurements was considered. It was found that the measured output instabilities are close to the average rms variance. The experimental results were utilized to estimate the rms instability at (1) a modulation frequency of 70 Hz and a sampling time of 2 μs and (2) at 285 Hz and 0.5 μs. The obtained instability was $\sim 1.0 \times 10^{-5}$ for both conditions.

References

1. M. Zanaveskin et al., "Correlation between the substrate roughness and light loss for interference mirror coatings," *Crystallogr. Rep.* **53**(4), 701–707 (2008).
2. D. Brodoceanu et al., "Femtosecond laser fabrication of high reflectivity micromirrors," *Appl. Phys. Lett.* **97**(4), 041104 (2010).
3. G. Berden, R. Peeters, and G. Meijer, "Cavity ring-down spectroscopy: experimental schemes and applications," *Int. Rev. Phys. Chem.* **19**(4), 565–607 (2000).
4. A. Zoeller et al., "Substantial progress in optical monitoring by intermittent measurement technique," *Proc. SPIE* **5963**, 56930D (2005).
5. E. F. Zalewski, "Radiometry and photometry," in *Handbook in Optics*, M. Bass, Ed., Vol. II, pp. 24.1–24.51, Optical Society of America, New York (1995).
6. V. Demkin and V. Privalov, *Methods for Power Stabilization of Continues Gas-Discharge Lasers*, Scientifically Research Institute of Electronics, Moscow (1986) (in Russian).
7. J. Ohtsubo, *Semiconductor Lasers. Stability, Instability and Chaos*, Springer, New York (2005).
8. W. Derksen, T. Monahan, and A. Lawes, "Automatic recording reflectometer for measuring diffuse reflectance in the visible and infrared regions," *J. Opt. Soc. Am.* **47**(11), 995–999 (1957).
9. R. Köhler, J. Luther, and J. Geist, "Reflectometer for measurements of scattering from photodiodes and other low scattering surfaces," *Appl. Opt.* **29**(21), 3130–3134 (1990).
10. E. R. Malamed, I. E. Putilov, and T. E. Tarasova, "Reflectometer," *Proc. SPIE* **6251**, 62510A (2006).
11. U. Gerhardt and G. Rubloff, "A normal incidence scanning reflectometer of high precision," *Appl. Opt.* **8**(2), 305–308 (1969).
12. W. Scott, L. Muldawer, and M. Graber, "Sensitive technique for measuring differences in reflectivity," *Appl. Opt.* **13**(8), 1956–1958 (1974).
13. L. Villanueva et al., "Automated precision reflectometer for first-surface mirrors II: system," *Proc. SPIE* **1323**, 316–326 (1990).
14. D. Aspnes and A. Studna, "High precision scanning ellipsometer," *Appl. Opt.* **14**(1), 220–228 (1975).
15. D. Zhuang and T. Yang, "Spectral reflectance measurements using a precision multiple reflectometer in the UV and VUV range," *Appl. Opt.* **28**(23), 5024–5028 (1989).
16. C. Castellini et al., "Characterization and calibration of a variable-angle absolute reflectometer," *Appl. Opt.* **29**(4), 538–543 (1990).
17. A. Gatesman, R. Giles, and J. Waldman, "High-precision reflectometer for submillimeter wavelengths," *J. Opt. Soc. Am. B* **12**(2), 212–219 (1995).
18. B. McGuckin et al., "Directional reflectance characterization facility and measurement methodology," *Appl. Opt.* **35**(24), 4827–4834 (1996).
19. L. Chen et al., "New design to measure absolute spectral reflectivity," *Opt. Eng.* **36**(4), 1169–1173 (1997).
20. A. Varaksin, Y. Polezhaev, and A. Polyakov, "Experimental investigation of the effect of solid particles on turbulent flow of air in a pipe," *High Temp.* **36**(5), 744–752 (1998).
21. V. Ya. Mendeleyev, "Scattering from unidirectional ground steel surfaces in the specular direction," *Opt. Commun.* **268**(1), 7–14 (2006).
22. H. Piombini and P. Voarino, "Apparatus designed for very accurate measurement of optical reflection," *Appl. Opt.* **46**(36), 8609–8618 (2007).
23. PerkinElmer Inc., "Lambda 800 and 900 spectrophotometer systems," http://www.surplusserver.com/PDF/Lambda800_900_Brochure.pdf (28 January 2014).
24. Varian Inc., "Cary 4000, 5000, and 6000i spectrophotometers," http://science.unitn.it/~semicon/members/pavesi/Technical%20Spec_87-1942.pdf (28 January 2014).

25. R. W. Larsen, *Introduction to MathCAD 2000*, Prentice Hall, Upper Saddle River, New Jersey (2001).
26. GOST 25786-83, "Lasers. Methods for measurements of average power and relative instability of average power," Gosstandart, Moscow (1983) (in Russian).
27. G. D. Burdun and B. N. Markov, *Principles of Metrology*, Standards, Moscow (1975) (in Russian).
28. D. W. Allan, J. H. Shoaf, and D. Halford, "Statistics of time and frequency data analysis," in *Time and Frequency. Theory and Fundamentals*, B. E. Blair, Ed., pp. 151–204, National Bureau of Standards, Boulder, Colorado (1974).

Vladimir Ya. Mendeleyev received a PhD in quantum electronics in 1988 from the Kharkov Radio Engineering Academy, USSR. He is currently working as a senior researcher in the laboratory for optical and thermophysical properties of materials of the Joint Institute for High Temperatures of the Russian Academy of Sciences. His research interests are in precision optical measurements, polarization and thermophysical properties of metals at high temperatures, and optical measurements of surface roughness.

Andrei V. Kourilovitch received a PhD in thermophysics in 2010 from the Joint Institute for High Temperatures of the Russian Academy of Sciences, where he is currently working as a senior researcher in the laboratory for optical and thermophysical properties of materials. His research interests are computer vision, optical remote sensing for on-line detection, and measurement of surface defects.